Nuclear Instruments and Methods in Physics Research A 677 (2012) 4–9

Contents lists available at SciVerse ScienceDirect

Nuclear Instruments and Methods in Physics Research A

journal homepage: www.elsevier.com/locate/nima

Designing an extended energy range single-sphere multi-detector neutron spectrometer

J.M. Gómez-Ros [a,b,*], R. Bedogni [b], M. Moraleda [a], A. Esposito [b], A. Pola [c], M.V. Introini [c], G. Mazzitelli [b], L. Quintieri [b], B. Buonomo [b]

[a] CIEMAT, Av. Complutense 40, 28040 Madrid, Spain
[b] IFNF-LNF, U.F. Fisica Sanitaria, via E. Fermi n. 40, 00044 Frascati, Italy
[c] Politecnico di Milano, Dipartimento di Energia, via Ponzio 34/3, 20133 Milano, Italy

ARTICLE INFO

Article history:
Received 11 November 2011
Received in revised form
16 February 2012
Accepted 22 February 2012
Available online 3 March 2012

Keywords:
Neutron spectrometry
Neutron dosimetry
Unfolding
Dysprosium foils

ABSTRACT

This communication describes the design specifications for a neutron spectrometer consisting of 31 thermal neutron detectors, namely Dysprosium activation foils, embedded in a 25 cm diameter polyethylene sphere which includes a 1 cm thick lead shell insert that degrades the energy of neutrons through (***n***,*x****n***) reactions, thus allowing to extension of the energy range of the response up to hundreds of MeV neutrons. The new spectrometer, called SP^2 (SPherical SPectrometer), relies on the same detection mechanism as that of the Bonner Sphere Spectrometer, but with the advantage of determining the whole neutron spectrum in a single exposure. The Monte Carlo transport code MCNPX was used to design the spectrometer in terms of sphere diameter, number and position of the detectors, position and thickness of the lead shell, as well as to obtain the response matrix for the final configuration. This work focuses on evaluating the spectrometric capabilities of the SP^2 design by simulating the exposure of SP^2 in neutron fields representing different irradiation conditions (test spectra). The simulated SP^2 readings were then unfolded with the FRUIT unfolding code, in the absence of detailed pre-information, and the unfolded spectra were compared with the known test spectra. The results are satisfactory and allowed approving the production of a prototypal spectrometer.

1. Introduction

Neutron fields ranging in energy from the thermal domain to tens or hundreds of MeV are a common characteristic to a number of facilities in the nuclear, medical, industrial or research fields. These neutron fields may be intentionally generated, as in nuclear plants or fast neutron irradiation facilities, or may be a parasitic effect, as in accelerator-based cancer therapy. Anyway, the measurement of these neutron fields is always desirable. The neutron energy being distributed over ten or more orders of magnitude, an accurate measurement cannot prescind from the knowledge of the neutron spectrum, thus requiring the use of a spectrometer that responds over such a broad energy interval. Of the many neutron spectrometry techniques available to the scientific community, only the Bonner Sphere Spectrometer (BSS) fulfils this requirement [1]. Whilst polyethylene spheres allow detecting neutrons up to 20 MeV, metal loaded spheres are needed when the neutron energy exceeds this value. The system that uses such modified spheres is called Extended Range Bonner Sphere Spectrometer (ERBSS) and is normally equipped with three or more spheres embedding lead, copper or tungsten inserts [2,3]. The ERBSS offers a number of advantages, chiefly the wide energy range, the isotropic response and the possibility to operate in broad ranges of intensities, photon background and beam time structures, by changing the central thermal neutron detector. On the contrary, significant disadvantages are: (1) the poor energy resolution [4], (2) the complex unfolding procedures, and (3) the need to sequentially expose the spheres, leading to lengthy measurements.

The practical importance of points (1) and (2) is normally limited, because neutron fields in workplaces can be usually modelled in terms of superposition of continuous structures, which are deducible from the physical phenomena at the basis of the neutron production mechanism. Fine structures like narrow peaks cannot be resolved, but their presence is usually known a priori and can be included as pre-information in the unfolding code. The impact of these disadvantages may be quantified by looking at the results of recent ERBSS comparisons. In this sense, the 2006 EC CONRAD comparison exercise [5], performed in the stray neutron field from a 400 MeV/*u* carbon ion beam (~30% of fluence above 20 MeV), showed that different ERBSS with different unfolding methods were able to provide compatible results in terms of total fluence

* Corresponding author at: CIEMAT, Av. Complutense 40, 28040 Madrid, Spain. Tel.: +34 913466000.
E-mail address: jm.gomezros@ciemat.es (J.M. Gómez-Ros).

0168-9002/$ - see front matter © 2012 Elsevier B.V. All rights reserved.
doi:10.1016/j.nima.2012.02.033

(differences in the order of 5%) or high-energy fluence (differences in the order of 10%). The larger differences observed in the high-energy domain are fully coherent with the limited degree of validation of the high-energy models adopted by the transport codes that are used to determine the response function of extended-range spheres. Improved agreements have been found when measuring the neutron field generated by a 62 MeV proton beam impinging on a PMMA phantom [6]. Therefore, point (3) constitutes the major difficulty for using BSS in operational scenarios, and certainly prevents the use of ERBSS as an in-line spectrometric monitor for neutron producing facilities.

The project NESCOFI@BTF (2011–2013), coordinated by INFN, attempts to design an in-line neutron spectrometer with the advantages of an ERBSS. The project plans to achieve this objective using a single extended range spherical moderator that embeds a number of active thermal neutron detectors in different positions. The development of such a device involves three main problems: setting up an array of miniaturised thermal neutron detectors to be read out in parallel, obtaining an isotropic response and extending the energy range up to hundreds of MeV.

Whilst the first question is currently under study, the last two problems are being investigated with Monte Carlo simulations and experimental prototypes based on passive detectors. The isotropic response can be achieved with an appropriate combination of the readings of the different detectors. This was demonstrated, either numerically or experimentally, by earlier studies on a 30 cm polyethylene sphere equipped with 43 detector positions symmetrically allocated along the three axes [7–9]. Pairs of thermoluminescent detectors (TLDs) ^{6}LiF and ^{7}LiF were firstly used to validate the response matrix calculated with Monte Carlo code MCNPX [10]. By averaging the readings of the TLDs (after photon subtraction) located at the same radial distance from the sphere centre, a nearly isotropic fluence response was obtained up to 20 MeV. Because of their relevant sensitivity to photons, TLDs have been replaced by Dysprosium activation foils in a further computational and experimental study [9]. After irradiation, the foils are counted in-situ using a portable beta counter. Owing to the high cross-section (2700 b at 0.025 eV) and the reasonably short half-life of ^{165}Dy (2.334 h), Dysprosium foils have been successfully used in operational measurements with ERBSS [11–15].

The extension in energy range above 20 MeV can be achieved by including a lead layer in the moderator, as described in Section 3. The new spectrometer, called SP^2 (SPherical SPectrometer), has been designed using the Monte Carlo transport code MCNPX to reduce the number of positions (31) and the external diameter (25 cm), determining also the number and distribution of the detectors and the position and thickness of the lead shell. In addition, MCNPX has been used to calculate the response matrix of the final configuration. As described below, the response of Dy foils has been modelled as thermal neutron detectors with the idea of building a passive prototype to experimentally check the spectrometer response matrix. This work evaluates the spectrometric capabilities of the SP^2 design by simulating the exposure of SP^2 in neutron fields representing different irradiation conditions (reference spectra) in a variety of workplaces, including high-energy fields. The simulated SP^2 readings have been unfolded with the FRUIT unfolding code [16,17], in the absence of detailed pre-information, and the unfolded spectra compared with the reference spectra. The results are satisfactory and allowed approving the production of a prototypal spectrometer based on Dy activation foils.

2. Materials and methods

Both the calculation of the response matrix and the simulation of neutron irradiations have been performed with the MCNPX 2.6 Monte Carlo code [10], using the ENDF/B-VII cross-section library [18] for neutrons with energies below 20 MeV and the room temperature cross-section tables in polyethylene, $S(\alpha,\beta)$. Response functions for neutrons with energies above 20 MeV were calculated using the Bertini intra-nuclear cascade model and the Dresner evaporation model [10,19]. A sufficiently large number of histories have been generated to obtain statistical uncertainties lower than 3% in all the cases.

The response of the of the Dy activation foils has been calculated as the number of ^{164}Dy(n,γ)^{165}Dy reactions within the foil volume normalised per unit incident fluence, using the track-length scoring option for the fluence (F4 tally), i.e.:

$$N_{(n,\gamma)} = \int dE \Phi_E V \rho_{at} \sigma_{(n,\gamma)} \quad (1)$$

where $\sigma_{(n,\gamma)}$ is the microscopic cross-section for (n,γ) reactions in Dy, V is the volume of the foil, ρ_{at} is the atomic density (atoms per unit volume), Φ_E is the energy distribution of neutron fluence, and $N_{(n,\gamma)}$ is the number of (n,γ) reactions in the considered volume. The Dy activation foils have diameter 1.2 cm, thickness 0.01 cm and purity higher than 99.9%. Density of the foils is 8.55 g cm^{-3}, thus giving $V\rho_{at}=3.553\times10^{-4}$ b^{-1} cm^{-1}.

The moderator materials are polyethylene, $(CH_2)_n$ 0.927 g cm^{-3} in density, and natural lead, 11.35 g cm^3. The isotopic compositions of lead (in weight fractions) are: 1.4% (^{204}Pb), 24.1% (^{206}Pb), 22.1% (^{207}Pb), and 52.4% (^{208}Pb).

3. Design specifications and calculated response matrix

The design of the instrument is based on the previous results for a 43-position, 30 cm diameter, polyethylene prototype [7–9]. The 43 positions were distributed as follows: 14 positions per axis, plus the central detector (common to the three axes). As discussed in the mentioned works, the use of the average reading, M_d, calculated for the detectors located at the same radial distance, d, permits obtaining a nearly isotropic response for a given energy spectrum, Φ_E, independently of the angular dependence.

In general, M_d can be expressed as follows [7]:

$$M_d = \int dE \Phi_E R_d(E) \quad (2)$$

where $R_d(E)$ is the average reading per unit incident fluence of the six detectors located at distance d from the centre of the sphere, as a function of the neutron energy. $R_d(E)$ is also called the "response function" for a given radial distance and angular distribution of the field. The considered spectrometer works under the following approximation:

$$R_d(E) \approx R_d^{(ISO)}(E) \quad (3)$$

where $R_d^{(ISO)}(E)$ is the spectrometer response function calculated for radial distance d and isotropic irradiation.

For the instrument based on a pure polyethylene sphere with 30 cm diameter [7–9], the response for neutron energies above 20 MeV is very poor. To increase the efficiency for high-energy neutrons, different configurations with a lead shell have been investigated. Finally, a new polyethylene sphere of radius 12.5 cm has been selected, replacing the material between 3.5 and 4.5 cm by a lead shell. One activation foil is located at the centre of the sphere, and 30 additional foils are symmetrically arranged along three perpendicular axes at five radial distances: 5.5, 7.5, 9.5, 11 and 12.5 cm (See Fig. 1). The six foils at 12.5 cm are located on the surface of the sphere, separated from the sphere by a 1 mm cadmium (Cd) layer, in order to estimate the thermal neutron

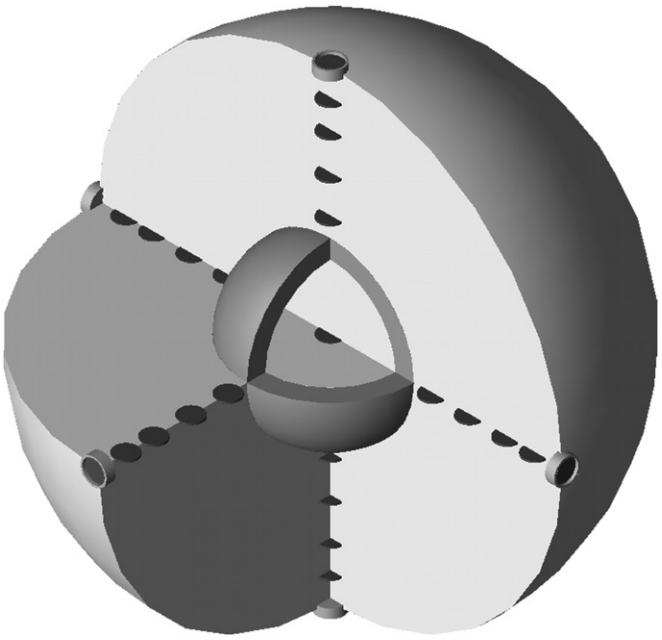

Fig. 1. Schematic view of the spectrometer showing the arrangement of the activation foils detectors along three perpendicular axes, as well as the inner lead layer.

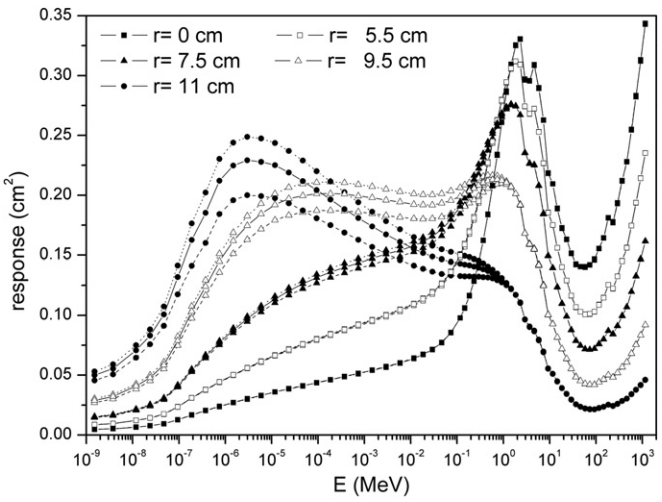

Fig. 2. Energy response functions to monoenergetic incident neutrons, averaged over the detectors located at the same distance from the centre, for three different irradiation geometries: along the (1 0 0) axis (dashed lines), isotropic (continuous lines), and along the (1 1 1) axis (dotted lines). The response functions have been calculated for radial distances 0, 5.5, 7.5, 9.5 and 11 cm.

component of the field. The Cd foil eliminates the contribution of neutrons backscattered from the sphere.

The response matrix has been calculated with MCNPX 2.6 [10] for 68 log-equidistant energies from 10^{-9} to 10^{3} MeV and three irradiation geometries: an isotropic irradiation and a parallel beam in two different incidence directions, namely (1 0 0) and (1 1 1) referred to the three perpendicular axis of detectors. Fig. 2 shows the energy dependence of the response functions, $R_{d,\vec{r}_0}(E)$, for the three irradiation geometries. Consistently with the results previously obtained with the 30 cm diameter polyethylene sphere, the lower and higher response values are obtained for the (1 0 0) and (1 1 1) irradiation, respectively. This effect is of practical importance only for the shallow detectors (d=11 cm and d=9.5 cm) and for energies in the keV region and below.

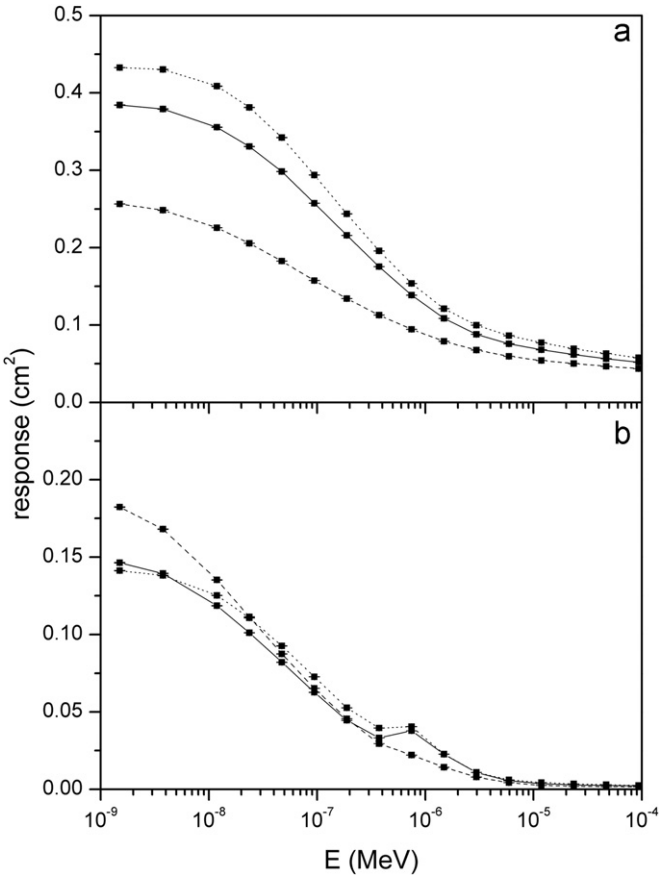

Fig. 3. Energy response function to monoenergetic incident neutrons, averaged over the detectors located on the surface of the sphere, for three different irradiation geometries: along the (1 0 0) axis (dashed lines), isotropic (continuous lines), and along the (1 1 1) axis (dotted lines): (a) without cadmium layer and (b) with cadmium.

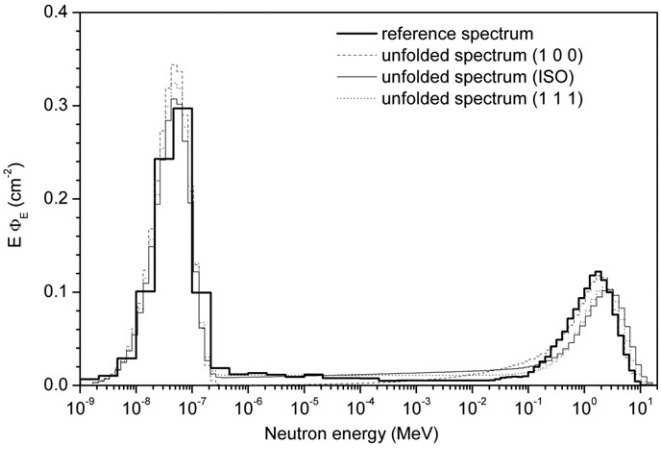

Fig. 4. Simulated exposure to a Fe+polyethylene moderated ^{252}Cf spectrum in three different irradiation geometries: along the (1 0 0) axis (dashed lines), isotropic (continuous lines), and along the (1 1 1) axis (dotted lines): (a) position profile, (b) unfolding results and (c) unfolding results with 8 extra positions at 14 cm from the centre of the sphere.

Because the three geometries give almost coincident response functions above 1 keV, the spectrometer response is practically isotropic in this energy domain. Moreover, the response functions above 10 MeV are significantly enhanced by the presence of the lead layer due to the (n,xn) reactions in lead, not only for the central detector but also for those located between 5.5 and 9.5 cm.

Table 1
Comparison between the integral quantities, Φ and $h^*(10)$, and fluence fractions derived from the reference iron and polyethylene moderated ^{252}Cf spectrum and those obtained by unfolding.

Irradiation Geometry	Total Fluence (cm^{-2})		$h^*(10)$ ($pSv\ cm^2$)		Fluence Fractions (%)					
	Reference	Unfolded	Reference	Unfolded	$E<0.4$ eV		0.4 eV $<E<$ 10 keV		10 keV $<E<$ 20 MeV	
					Reference	Unfolded	Reference	Unfolded	Reference	Unfolded
100	1	1.00 ± 0.01	112	113 ± 5	30.0	39.5	40.1	28.0	29.9	32.5
ISO	1	1.01 ± 0.01	112	108 ± 5	30.0	35.1	40.1	35.1	29.9	29.8
111	1	1.05 ± 0.03	112	103 ± 8	30.0	37.0	40.1	35.9	29.9	27.1

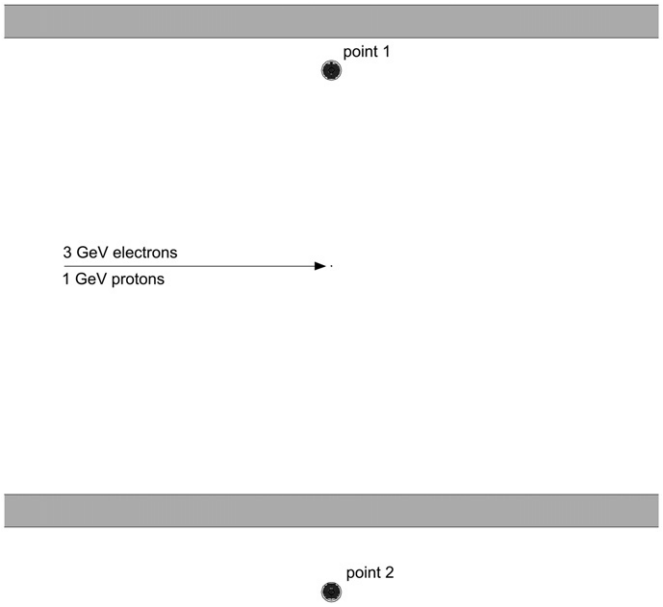

Fig. 5. Schematic view of the geometry used to simulate the exposure to high energy neutron field.

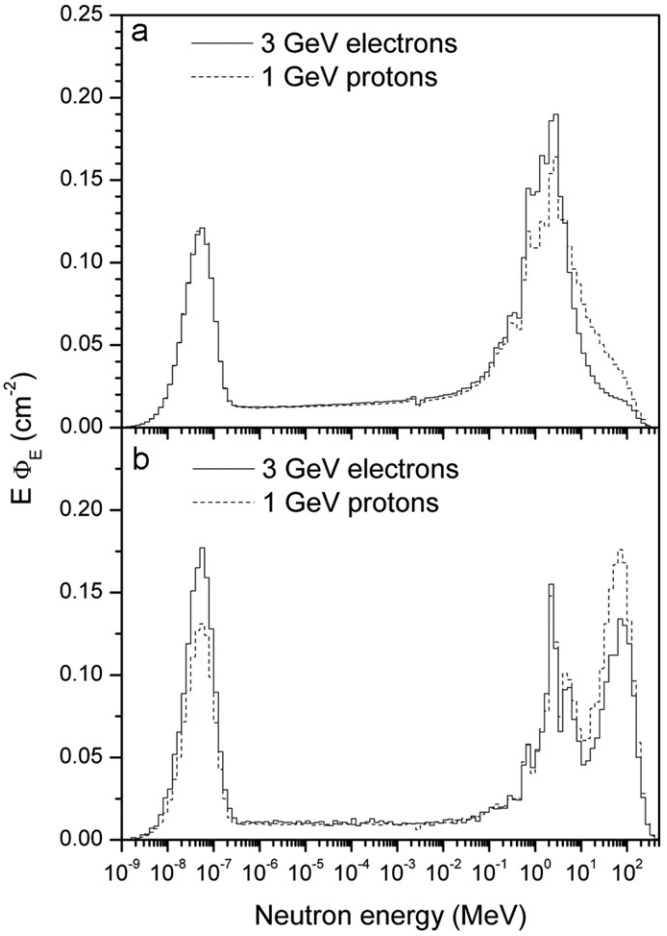

Fig. 6. Simulated high energy neutron spectra calculated according to the geometry depicted in Fig. 5.

As it can be seen, the response above 1 MeV for fast and high energy neutrons is completely isotropic. According to the response matrix displayed in Fig. 2, a good spectrometric performance is expected above 1 keV.

Fig. 3(a) and (b) motivates the choice of protecting the superficial detectors ($d=12.5$ cm) from the sphere backscatter, using a Cd filter. In Fig. 3(a) the response functions for $d=12.5$ cm in the absence of Cd are showed. As expected, the functions obtained in different geometries are very different, especially from 1 meV to 1 eV. By introducing the Cd filter (Fig. 3b), the variability interval is significantly reduced, from $\pm30\%$ (relative to the mean value, at 0.01 eV) to 8%.

4. Unfolding tests

A set of irradiation exposures to neutron spectra was simulated with MCNPX to evaluate the performance of the spectrometer. The readings (number of capture reactions in the Dy foils) of the detectors located at the same radial position were averaged and used as input data for the unfolding code. The Cd filtered configuration was adopted for the detectors at $d=12.5$ cm.

Based on experimental experience with Dyfoils [9,11–15], the combination of the uncertainty of the foil readings and of the overall uncertainty of the response matrix was assumed to be 3%. The FRUIT code was used in parametric mode [16], that is to say that neutron spectrum is modelled as the superposition of elementary functions, covering the different energy domains and fully described by a reduced number (around ten) of physically meaningful parameters. FRUIT is designed as a tool for operational measurements where very few pre-information is available. Besides the sphere response functions, the counts and related uncertainties, FRUIT requires only introduction of qualitative information on the type of "radiation environment" on the basis of a check-box input section. The code randomly generates a default spectrum needed to start the iterative procedure, on the basis of the radiation environment selected by the user. Taking advantage of a flexible tolerance convergence mechanism, results do not depend on the numerical values of this spectrum.

The code includes a statistics tool to derive the probability distributions of all quantities related to the final spectrum: the parameters, the fluence (and fractions of fluence in given energy intervals), the ambient dose equivalent and the numerical values of the neutron spectrum, specified bin by bin. Uncertainties are

derived by considering these probability distributions. Uncertainties of input quantities (sphere counts, response matrix and other sources that may randomly affect the sphere counts) are used to perform these analyses.

Different test spectra, all normalised to the unit fluence, were chosen to represent the operational irradiation conditions, as explained below. In all the cases, the response matrix calculated under isotropic irradiation condition was used.

(1) *Nuclear plant workplace spectrum*. This was simulated, according to IAEA [20] with a ^{252}Cf source moderated with 5 cm of iron and 10 cm of polyethylene. The spectrum contains a significant amount of thermal neutrons. Three different irradiation geometries were used: isotropic, (1 0 0) and (1 1 1). The unfolded spectra are compared with the test spectrum in Fig. 4. Unfolding uncertainties, not reported for a better readability, are fully comparable with the small differences between the three unfolded spectra. The unfolded spectra are comparable and agree well with the reference spectrum, even in the thermal region, thus confirming the effectiveness of the Cd-filtered configuration in order to obtain an isotropic response even for thermal neutrons. The agreement between unfolded and reference spectra is quantified in Table 1, where the following spectrum-integrated quantities are reported: total neutron fluence; spectrum-average fluence-to-ambient dose equivalent conversion coefficient, $h^*(10)$, fractions of fluence in the thermal ($E < 0.4$ eV), epithermal (0.4 eV $< E <$ 10 keV) and fast ($E >$ 10 keV) domain.

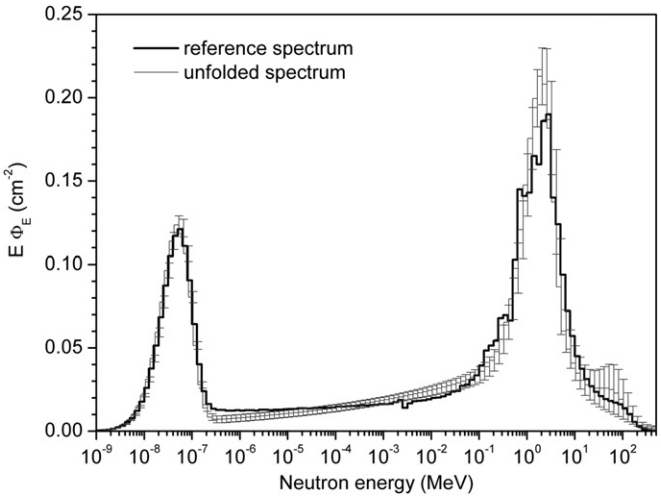

Fig. 7. Simulated exposure to a high energy neutron field (unshielded high energy electron source).

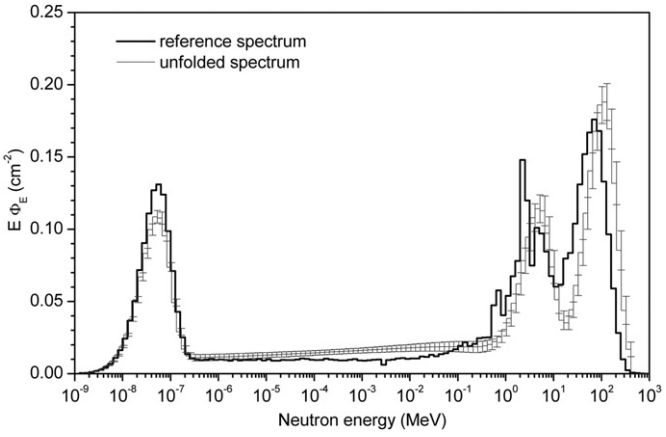

Fig. 8. Simulated exposure to a high energy neutron field (shielded high energy proton source).

(2) *High energy spectra.* Neutron spectra representative of the workplaces in high-energy electron or proton accelerators have been calculated using the simplified model suggested in [17]. The neutron producing target was simulated by a 1 cm radius iron sphere located at the centre of a 8 m diameter cylindrical tunnel with 50 cm thick concrete walls (Fig. 5). Collimated primary beams of 3 GeV electrons or 1 GeV protons were used. The neutron spectra have been calculated at two locations: point 1 located inside the cylinder at 3 m from the target (unshielded spectrum), and point 2 outside the cylinder, at 5 m distance from the target (concrete-shielded spectrum), as shown in Fig. 6. As expected, the "unshielded" spectra are dominated by the evaporative component, whilst in the concrete-shielded spectra this component is accompanied by a relevant high-energy peak located at about 10 MeV. Because the spectra for a given shielding configuration are practically particle-independent, the unfolding tests were performed only for electrons in unshielded condition, and for protons in shielded condition. The *high-energy accelerator* models of FRUIT have been used. The unfolded spectra with bin-per-bin uncertainty bars are shown in Figs. 7 and 8 and the integral quantities are reported in Table 2.

5. Conclusions

This work demonstrates that a single moderating sphere, including a 1 cm lead layer and embedding 31 thermal neutron detectors symmetrically arranged along the three axes, can provide nearly isotropic fluence response and has spectrometric capabilities for neutrons in the energy range from thermal up to hundreds of MeV. These properties have been numerically verified by simulating the exposure of the device to the neutron fields corresponding to different operational workplaces and using the FRUIT code for unfolding. In all cases, the unfolded data agree with the reference spectra in terms of spectrum shape and spectrum-integrated quantities, even in restricted energy subintervals (thermal, epithermal, fast and high-energy), within

Table 2
Comparison between the integral quantities, Φ and $h^*(10)$, and fluence fractions derived from the reference high energy spectra and those obtained by unfolding.

Neutron Spectrum		Total Fluence (cm^{-2})	$h^*(10)$ ($pSv\ cm^2$)	Fluence Fractions (%)			
				$E < 0.4$ eV	0.4 eV $< E <$ 10 keV	10 keV $< E <$ 20 MeV	$E >$ 20 MeV
High-E electrons unshielded point	Reference	1	216	12.6	26.2	57.2	4.0
	Unfolded	0.98 ± 0.02	218 ± 11	14.0	24.2	56.9	4.9
High-E protons shielded point	Reference	1	247	12.8	21.8	35.1	30.3
	Unfolded	1.07 ± 0.05	238 ± 15	11.6	22.9	29.5	36.0

unfolding uncertainties. The response matrix obtained for isotropic irradiation is suited for all the scenarios investigated in this work. The spectrometric performance is adequate even in energy regions where the instrument can be affected by poor energy resolution ($E > 20$ MeV) or by anisotropy effects (thermal neutrons). The Cd-filtering technique applied to the superficial detectors ($d = 12.5$ cm) allows to accurately estimation of the thermal fluence.

Acknowledgements

This work has been partially supported by projects AIC10-D-000570 (MICINN, Spain) and the INFN-CSN5 (Commissione Scientifica Nazionale 5) project NESCOFI@BTF.

References

[1] D.J. Thomas, Radiation Measurements 45 (2010) 1178.
[2] B. Wiegel, A.V. Alevra, Nuclear Instruments and Methods in Physics Research A 476 (2002) 36.
[3] A. Esposito, R. Bedogni, C. Domingo, M.J. Garcia, K. Amgarou, Radiation Measurements 45 (2010) 1522.
[4] M. Reginatto, Nuclear Instruments and Methods in Physics Research A 480 (2002) 690.
[5] B. Wiegel, S. Agosteo, R. Bedogni, M. Caresana, A. Esposito, G. Fehrenbacher, M. Ferrarini, E. Hohmann, C. Hranitzky, A. Kasper, S. Khurana, V. Mares, M. Reginatto, S. Rollet, W. Rühm, D. Schardt, M. Silari, G. Simmer, E. Weitzenegger, Radiation Measurements 44 (2009) 660.
[6] K. Amgarou, R. Bedogni, C. Domingo, A. Esposito, A. Gentile, G. Carinci, S. Russo, Nuclear Instruments and Methods in Physics Research A 654 (2011) 399.
[7] J.M. Gómez-Ros, R. Bedogni, M. Moraleda, A. Delgado, A. Romero, A. Esposito, Nuclear Instruments and Methods in Physics Research A 613 (2010) 127.
[8] J.M. Gómez-Ros, R. Bedogni, M. Moraleda, A. Romero, A. Delgado, A. Esposito, Radiation Measurements 45 (2010) 1220.
[9] D.B. Pelowitz (Ed.), MCNPX User's Manual Version 2.6, Report LA-CP-07-1473, 2008.
[10] J.M. Gómez-Ros, R. Bedogni, I. Palermo, A. Esposito, A. Delgado, M. Angelone, M. Pillon, Radiation Measurements 46 (2011) 1712.
[11] R. Bedogni, P. Ferrari, G. Gualdrini, A. Esposito, Radiation Measurements 45 (2010) 1201.
[12] R. Bedogni, A. Esposito, J.M. Gómez-Ros, Radiation Measurements 45 (2010) 1205.
[13] R. Bedogni, A. Esposito, C. Andreani, R. Senesi, M.P. de Pascale, P. Picozza, A. Pietropaolo, G. Gorini, C.D. Frost, S. Ansell, Nuclear Instruments and Methods in Physics Research A 612 (2009) 143.
[14] R. Bedogni, A. Esposito, A. Gentile, M. Angelone, M. Pillon, Radiation Measurements 46 (2011) 1757.
[15] R. Bedogni, L. Quintieri, B. Buonomo, A. Esposito, G. Mazzitelli, L. Foggetta, J.M. Gómez-Ros, Nuclear Instruments and Methods in Physics Research A 659 (2011) 373.
[16] R. Bedogni, C. Domingo, A. Esposito, F. Fernández, Nuclear Instruments and Methods in Physics Research A 580 (2007) 1301.
[17] R. Bedogni, M. Pelliccioni, A. Esposito, Nuclear Instruments and Methods in Physics Research A 615 (2010) 78.
[18] M.B. Chadwick, P. Oblozinsky, M. Herman, et al., Nuclear Data Sheets 107 (2006) 2931.
[19] C. Pioch, V. Mares, W. Rühm, Radiation Measurements 45 (2010) 1263.
[20] International Atomic Energy Agency (IAEA), Technical Reports Series No. 403, Vienna, 2001.